



Cite this: DOI: 10.1039/c8dt01755g

Received 2nd May 2018,

Accepted 16th July 2018

DOI: 10.1039/c8dt01755g

rsc.li/dalton

## A Mn<sub>13</sub>-cluster based coordination polymer as a co-catalyst of CdS for enhanced visible-light driven H<sub>2</sub> evolution†

Tian Wen,<sup>a</sup> Lei Zhang \*<sup>a</sup> and Wolfgang Schmitt <sup>b</sup>

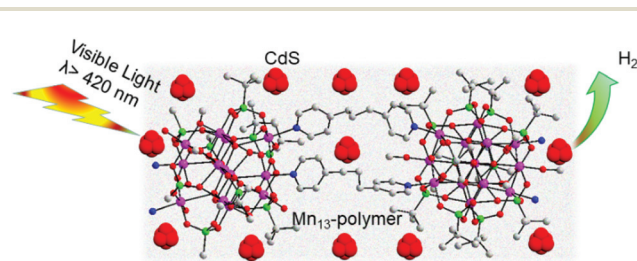
**A coordination cluster-based polymer was used for the first time as a noble-metal-free co-catalyst of CdS, giving rise to significantly enhanced photocatalytic H<sub>2</sub> production. This work demonstrates the feasibility of cluster materials in assembling highly-active and low-priced photocatalysts.**

Photocatalytic water-splitting H<sub>2</sub> production is considered to be a promising solution for the global energy and environmental crisis. In the past few decades, semiconductor photocatalysts, especially metal sulfides (*e.g.* CdS), have been intensively studied due to their advantageous characteristics such as low cost, facile preparation and excellent visible light response.<sup>1–5</sup> Despite some tremendous achievements, the activities and applications of pure metal sulfides are still greatly obstructed due to the fast recombination of photogenerated electron–hole pairs. To overcome this obstruction, the use of co-catalyst composites has proven to be a successful method for improving the efficiency and stability of semiconductor photocatalysts.<sup>6–9</sup> However, the most active H<sub>2</sub> evolution co-catalysts are usually expensive and involve scarce noble metals (*e.g.* Pt), greatly limiting the practical applications of these photocatalytic systems. Therefore, the development of inexpensive and active co-catalysts remains a great challenge for the future to establish large-scale photocatalytic H<sub>2</sub> production.

Recently, several Earth-abundant co-catalyst systems for semiconductor-based H<sub>2</sub> evolution have been studied, involving transition metal oxides, sulfides and carbides.<sup>10–13</sup> In particular, the use of porous materials and assemblies of titanium-oxo clusters can also greatly increase the CdS-derived H<sub>2</sub> production.<sup>14–16</sup> On the other hand, inspired by the catalytically active Mn<sub>4</sub>CaO<sub>5</sub> cubane cluster in PS II, several Mn-oxo complexes have been investigated as photocatalysts to promote

the water oxidation reaction to produce O<sub>2</sub>.<sup>17</sup> However, to the best of our knowledge the application of Mn-oxo clusters as co-catalysts for H<sub>2</sub> production has not yet been investigated.

In this work, to explore the use of a new Earth-abundant co-catalyst for hydrogen evolution from H<sub>2</sub>O, we loaded CdS nanoparticles to a porous Mn<sub>13</sub>-cluster based coordination polymer and tested the corresponding photocatalytic performances (Scheme 1).<sup>18</sup> The main reasons of selecting this Mn<sub>13</sub>-type material are as follows: (i) this coordination polymer is highly porous and characterised by large voids (and defined hydrophilic channels) (Fig. S2†); (ii) the Mn<sub>13</sub> building units present labile Jahn–Teller sites that can be used for guest exchange (possible water absorption); (iii) the red/brown-coloured crystals of the Mn<sub>13</sub>-polymer may further increase the efficiency of the visible light absorption; and (iv) the Mn<sub>13</sub>-polymer containing distinctive, well-distributed electronegative atoms (P and N) might facilitate enhanced electronic coupling with the CdS particles. Prior to the catalytic test reactions, the obtained Mn<sub>13</sub>-polymer/CdS composites were well characterized by transmission electron microscopy (TEM) and related photochemical analysis. In comparison with pure CdS catalysts under visible-light irradiation, these composite catalysts displayed a significantly enhanced H<sub>2</sub> evolution activity. Furthermore the activity is dependent on the amount of the loaded Mn<sub>13</sub>-polymer whereby samples that contain 7 wt% Mn<sub>13</sub>-polymer give the highest H<sub>2</sub> production reaching values of 3600 μmol h<sup>−1</sup> g<sup>−1</sup>.



**Scheme 1** The illustration of an idealized assembly of the Mn<sub>13</sub>-polymer/CdS composites. Red, O; green, P; gray, C; blue, N; pink, Mn.

<sup>a</sup>School of Chemistry, The University of Melbourne, Parkville, Victoria 3010, Australia. E-mail: lei.zhang1@unimelb.edu.au

<sup>b</sup>School of Chemistry & CRANN, University of Dublin, Trinity College, Dublin 2, Ireland

† Electronic supplementary information (ESI) available: Materials, synthesis and physical measurements. See DOI: 10.1039/c8dt01755g

In the crystal structure of the selected Mn<sub>13</sub>-polymer, the 1D chains with positive charges assembled from Mn<sub>13</sub>-oxo clusters and 4,4'-trimethylenedipyridine ligands are packed together to form a porous architecture.<sup>18</sup> It has already been well established that such supramolecular channels can be used for guest pass ways (Fig. S2†). A simple and effective mechanical grinding method was then applied involving a freshly produced Mn<sub>13</sub>-polymer and CdS nanoparticles to produce effective catalysts for the photocatalytic H<sub>2</sub>-production. Firstly, the successful synthesis of the CdS nanoparticles (NPs) was corroborated by TEM and powder X-ray diffraction (PXRD) analyses (Fig. S3 and S4†). Then, the pristine samples of the Mn<sub>13</sub>-polymer and CdS were mixed in an agate mortar and ground for *ca.* 30 min (see the ESI† for details). The TEM images (Fig. 1a–b), energy dispersive X-ray (EDX) spectra (Fig. S5†) and EDX elemental mapping images (Fig. 1c) of the finer fraction imply that the Mn<sub>13</sub>-polymer was successfully loaded onto the surface of the CdS nanoparticles *via* electrostatic interactions to give homogeneous samples of Mn<sub>13</sub>-polymer/CdS.

The photocatalytic water-splitting H<sub>2</sub> production experiments were performed using a white-light emitting-diode (LED) as the light source and Mn<sub>13</sub>-polymer/CdS composites as catalysts at room temperature, along with triethanolamine (TEOA 16 vol%) as a sacrificial reagent. For comparative studies, samples with various Mn<sub>13</sub>-polymer loadings were applied. Remarkably, the coupling of the Mn<sub>13</sub>-polymer with CdS indeed leads to an enhancement in the photocatalytic activity. As displayed in Fig. 2a, pristine CdS showed a very low photocatalytic activity, producing 680 μmol h<sup>-1</sup> g<sup>-1</sup> of H<sub>2</sub>. When a small quantity of the Mn<sub>13</sub>-polymer (2.4 wt%) was

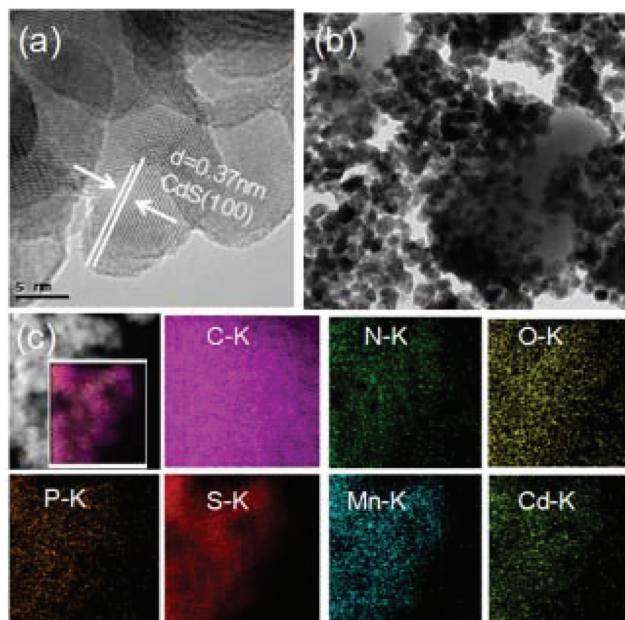


**Fig. 1** (a) HRTEM image of CdS nanoparticles. (b) The typical TEM image of samples of the Mn<sub>13</sub>-polymer/CdS. (c) The EDX mapping images of samples of the Mn<sub>13</sub>-polymer/CdS.

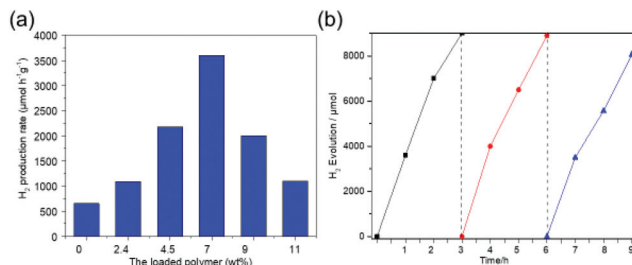


**Fig. 2** (a) Mn<sub>13</sub>-polymer loading amount dependent photocatalytic H<sub>2</sub> evolution activities of the Mn<sub>13</sub>-polymer/CdS. (b) Stability test of 7 wt% Mn<sub>13</sub>-polymer/CdS with prolonged visible light irradiation for 9 h.

loaded, the H<sub>2</sub> production was greatly increased to 1090 μmol h<sup>-1</sup> g<sup>-1</sup>. Then, by increasing the loading of the Mn<sub>13</sub>-polymer, the photocatalytic activities of the obtained Mn<sub>13</sub>-polymer/CdS samples were gradually enhanced. Using the optimal loading of the 7.0 wt% Mn<sub>13</sub>-polymer, the corresponding Mn<sub>13</sub>-polymer/CdS composite gave the highest photocatalytic H<sub>2</sub> production rate of 3600 μmol h<sup>-1</sup> g<sup>-1</sup>, exceeding about 5 times that of bare CdS.

It has been recently proven that the hetero-structured photocatalysts could successfully enhance the activity of H<sub>2</sub> production by binding different building blocks through electrostatic interactions.<sup>19–24</sup> Therefore, the superior activity of the investigated Mn<sub>13</sub>-polymer/CdS composites may be ascribed to the combination between CdS and the Mn<sub>13</sub>-polymer, which greatly facilitates a rapid interfacial charge transfer. Interestingly, a further increase in the loading of the Mn<sub>13</sub>-polymer leads to an obvious decrease of the photocatalytic activity. It is noteworthy that the pure Mn<sub>13</sub>-polymer displayed no activity towards H<sub>2</sub> production, whilst its PXRD pattern remained unchanged under the corresponding experimental conditions, highlighting the stability of the co-catalyst under visible light illumination (Fig. S1†). So, one can expect that excess Mn<sub>13</sub>-polymer co-catalysts block the active surface sites and impede the light absorption of the CdS catalyst. Moreover, the obtained Mn<sub>13</sub>-polymer/CdS composites are characterized by relatively high photocatalytic stability (Fig. 2b). These results suggest that the Mn<sub>13</sub>-polymer is an excellent co-catalyst for CdS in order to significantly promote its photocatalytic H<sub>2</sub> production.

To further characterize the obtained Mn<sub>13</sub>-polymer/CdS catalysts and gain some mechanistically insight into the above described H<sub>2</sub> production, additional photochemical studies were carried out. Firstly, the light harvesting capabilities of the CdS nanoparticles, the Mn<sub>13</sub>-polymer, and their composites were tested by UV-Vis diffuse reflectance spectroscopy (Fig. 3a). The fresh Mn<sub>13</sub>-polymer showed strong light absorption between 400 and 800 nm. Thus, the light absorption characteristics of the Mn<sub>13</sub>-polymer/CdS composites became more pronounced in the region of 550–800 nm in comparison with the pure CdS materials. However, the absorption edge of the Mn<sub>13</sub>-polymer/CdS showed no significant shift compared to CdS, indicating that doping effects, whereby electron-rich non-

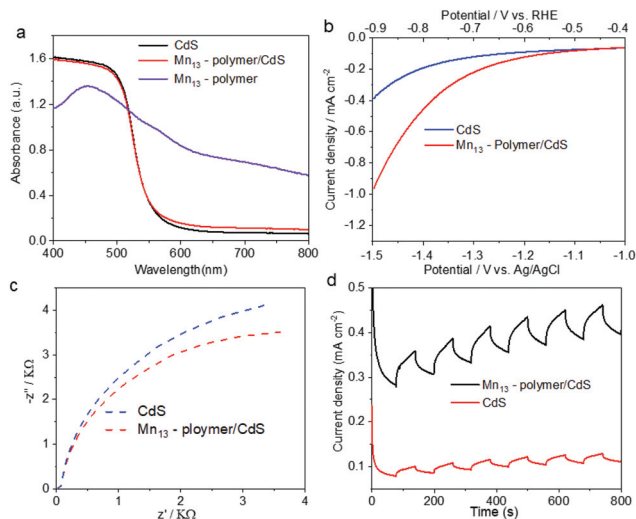


**Fig. 3** (a) Ultraviolet–visible absorption spectra of CdS, Mn<sub>13</sub>-polymer, and Mn<sub>13</sub>-polymer/CdS. (b) Polarization curves of sample electrodes in 0.5 M Na<sub>2</sub>SO<sub>4</sub> solution. (c) EIS Nyquist plots of CdS and Mn<sub>13</sub>-polymer/CdS electrodes measured under the open-circle potential and visible-light irradiation in 0.5 M Na<sub>2</sub>SO<sub>4</sub>. (d) The transient photocurrent responses of CdS and Mn<sub>13</sub>-polymer/CdS electrodes in 0.2 M Na<sub>2</sub>S + 0.04 M Na<sub>2</sub>SO<sub>3</sub> mixed aqueous solution under visible-light irradiation.

metallic elements such as N, O and P are incorporated into the crystal structure of CdS, do not occur. Similar characteristics were also observed for various Mn<sub>13</sub>-polymer loadings (Fig. S6<sup>†</sup>), thus confirming the structural stability of CdS in the catalyst composites. Furthermore, electrochemical measurements and X-ray photoemission spectroscopy (XPS) studies were carried out to investigate the charge separation and transfer. As can be seen from the polarization curves shown in Fig. 3b, the Mn<sub>13</sub>-polymer/CdS composite shows a remarkably smaller onset potential than CdS for an electrocatalytic HER. Moreover, as compared to pure CdS, the Mn<sub>13</sub>-polymer/CdS composite also features a smaller semicircle in electrochemical impedance spectroscopy (EIS; Fig. 3c), indicating faster interfacial electron transfer. To achieve such a rapid interfacial charge transfer between the Mn<sub>13</sub>-polymer and CdS, the formation of strong electronic interactions is essential. The XPS spectrum of the Mn<sub>13</sub>-polymer/CdS composite shows two peaks located at 406.61/411.35 eV and 160.90/162.02 eV attributed to Cd 3d<sub>5/2</sub>/Cd 3d<sub>3/2</sub> and S 2P<sub>3/2</sub>/S 2P<sub>1/2</sub>, respectively. Clearly, these signals of Mn<sub>13</sub>-polymer/CdS samples have been lowered by *ca.* 0.21–0.23 and 0.29–0.34 eV compared to pristine CdS samples, respectively, confirming relatively strong electronic coupling between the Mn<sub>13</sub>-polymer and the CdS nanoparticles (Fig. S7 and S8<sup>†</sup>). Thus, the direct electron transfer from CdS to the Mn<sub>13</sub>-polymer upon respective combination can be expected. It seems reasonable to assume that the *tert*-butylphosphonate and the 4,4'-trimethylenedipyridine ligands that locate at the periphery of the Mn<sub>13</sub>-polymer interact with the CdS nanoparticles whereby electronegative atoms with lone pairs, *e.g.* the P and N atoms provide pathways for electron transport. Consequently, this strong electronic coupling

arises from a weak electronic push–pull effect between the CdS and Mn<sub>13</sub>-polymer components. This effect involving electro-negative ligand-atoms may be further facilitated by complementary charges of the polymer and the surface charges of the CdS particles, thus contributing to the effective interfacial charge separation and transfer in the Mn<sub>13</sub>-polymer/CdS system. Finally, transient photocurrent (TPC) spectroscopy was applied to interpret the charge-carrier separation and transfer efficiency. As shown in Fig. 3d, the TPC value was significantly increased after the Mn<sub>13</sub>-polymer loading, further confirming that the efficiency of charge separation is greatly improved in the composite material.

In conclusion, for the first time, Mn coordination clusters have been applied as highly active noble-metal-free co-catalysts facilitating enhanced visible-light driven H<sub>2</sub> evolution in the presence of CdS. Taking the advantage of a convenient mechanical grinding strategy, a series of Mn<sub>13</sub>-polymer/CdS composite catalysts were prepared. Interestingly, the combination of the Mn<sub>13</sub>-polymer and CdS nanoparticles resulted in enhanced photocatalytic H<sub>2</sub> production activities which were highly dependent on the loading quantities of the Mn<sub>13</sub>-polymer. It was also demonstrated that the photocatalytic activity of the Mn<sub>13</sub>-polymer/CdS system stems from the intimate electrostatic interaction between the Mn<sub>13</sub>-polymer and CdS NPs, thus facilitating efficient charge mobility. Therefore, this work highlights the potential of Mn coordination clusters as low-cost co-catalysts for the photocatalytic H<sub>2</sub> production. The presented system points towards alternatives to noble metal catalysts and highlights new opportunities for the construction of hetero-structural materials towards energy related applications.

## Conflicts of interest

There are no conflicts of interest to declare.

## Acknowledgements

This work is supported by the Australian Research Council (DE150100901). The authors also thank the Science Foundation Ireland (SFI; 13/IA/1896) and the European Research Council (SURAMOL CoG 2014–647719).

## References

- 1 J. Ran, J. Zhang, J. Yu, M. Jaroniec and S. Z. Qiao, *Chem. Soc. Rev.*, 2014, **43**, 7787.
- 2 J. Ran, T. Y. Ma, G. Gao, X.-W. Du and S. Z. Qiao, *Energy Environ. Sci.*, 2015, **8**, 3708.
- 3 W.-J. Ong, L.-L. Tan, Y. H. Ng, S.-T. Yong and S.-P. Chai, *Chem. Rev.*, 2016, **116**, 7159.
- 4 Q. Wang, T. Hisatomi, Q. Jia, H. Tokudome, M. Zhong, C. Wang, Z. Pan, T. Takata, M. Nakabayashi, N. Shibata,

- Y. Li, I. D. Sharp, A. Kudo, T. Yamada and K. Domen, *Nat. Mater.*, 2016, **15**, 611.
- 5 P. Zhang, T. Wang, X. Chang and J. Gong, *Acc. Chem. Res.*, 2016, **49**, 911.6.
- 6 J. Yang, D. Wang, H. Han and C. Li, *Acc. Chem. Res.*, 2013, **46**, 1900.
- 7 J. Chen, X.-J. Wu, L. Yin, B. Li, X. Hong, Z. Fan, B. Chen, C. Xue and H. Zhang, *Angew. Chem., Int. Ed.*, 2015, **54**, 1210.
- 8 D. Zheng, X.-N. Cao and X. Wang, *Angew. Chem., Int. Ed.*, 2016, **55**, 11512.
- 9 P. Zhang, T. Wang, X. Chang and J. Gong, *Acc. Chem. Res.*, 2016, **49**, 911.
- 10 J. Ran, G. Gao, F.-T. Li, T.-Y. Ma, A. Du and S.-Z. Qiao, *Nat. Commun.*, 2017, **8**, 13907.
- 11 J. Ran, J. G. Yu and M. Jaroniec, *Green Chem.*, 2011, **13**, 2708.
- 12 Y. Zhou, L. Zhang, J. Liu, X. Fan, B. Wang, M. Wang, W. Ren, J. Wang, M. Li and J. Shi, *J. Mater. Chem. A*, 2015, **3**, 3862.
- 13 F. Dong, Z. Zhao, T. Xiong, Z. Ni, W. Zhang, Y. Sun and W. K. Ho, *ACS Appl. Mater. Interfaces*, 2013, **5**, 11392.
- 14 Y. Liu, Q. P. Lin, Q. C. Zhang, X. H. Bu and P. Y. Feng, *Chem. – Eur. J.*, 2014, **20**, 8297.
- 15 D. W. Jing and L. J. Guo, *J. Phys. Chem. B*, 2006, **110**, 11139.
- 16 Z. Q. Jiang, J. X. Liu, M. Y. Gao, X. Fan, L. Zhang and J. Zhang, *Adv. Mater.*, 2017, **29**, 1603369.
- 17 H. J. M. Hou, *Materials*, 2011, **4**, 1693.
- 18 L. Zhang, R. Clérac, C. I. Onet, M. Venkatesan, P. Heijboer and W. Schmitt, *Chem. – Eur. J.*, 2012, **18**, 13984.
- 19 H. Wang, L. Zhang, Z. Chen, J. Hu, S. Li, Z. Wang, J. Liu and X. Wang, *Chem. Soc. Rev.*, 2014, **43**, 5234.
- 20 K. Chang, Z. Mei, T. Wang, Q. Kang, S. Ouyang and J. Ye, *ACS Nano*, 2014, **8**, 7078.
- 21 J. Hu, A. Liu, H. Jin, D. Ma, D. Yin, P. Ling, S. Wang, Z. Lin and J. Wang, *J. Am. Chem. Soc.*, 2015, **137**, 11004.
- 22 J. Chen, X.-J. Wu, L. Yin, B. Li, X. Hong, Z. Fan, B. Chen, C. Xue and H. Zhang, *Angew. Chem., Int. Ed.*, 2015, **54**, 1210.
- 23 Y. Chen, S. Zhao, X. Wang, Q. Peng, R. Lin, Y. Wang, R. Shen, X. Cao, L. Zhang, G. Zhou, J. Li, A. Xia and Y. Li, *J. Am. Chem. Soc.*, 2016, **138**, 4286.
- 24 M. Liu, Y. Chen, J. Su, J. Shi, X. Wang and L. Guo, *Nat. Energy*, 2016, **1**, 16151.